Dear Author,

Please, note that changes made to the HTML content will be added to the article before publication, but are not reflected in this PDF.

Note also that this file should not be used for submitting corrections.

AUTHOR QUERY FORM

ELSEVIER **Journal: MSC** **Article Number: 5099**	**Please e-mail or fax your responses and any corrections to:** **Karthikeyan Arivazhagan** **E-mail: Corrections.ESIL@elsevier.spitech.com** **Fax: +1 619 699 6721**

Dear Author,

Please check your proof carefully and mark all corrections at the appropriate place in the proof (e.g., by using on-screen annotation in the PDF file) or compile them in a separate list. Note: if you opt to annotate the file with software other than Adobe Reader then please also highlight the appropriate place in the PDF file. To ensure fast publication of your paper please return your corrections within 48 hours.

For correction or revision of any artwork, please consult http://www.elsevier.com/artworkinstructions.

We were unable to process your file(s) fully electronically and have proceeded by

☐ Scanning (parts of) your article   ☐ Rekeying (parts of) your article   ☐ Scanning the artwork

Any queries or remarks that have arisen during the processing of your manuscript are listed below and highlighted by flags in the proof. Click on the 'Q' link to go to the location in the proof.
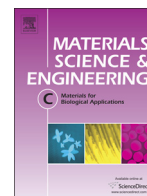
Location in article	Query / Remark: click on the Q link to go Please insert your reply or correction at the corresponding line in the proof
Q1	Please confirm that given names and surnames have been identified correctly.
Q2	Your article is registered as a regular item and is being processed for inclusion in a regular issue of the journal. If this is NOT correct and your article belongs to a Special Issue/Collection please contact k.arivazhagan@elsevier.com immediately prior to returning your corrections.
Q3	Supplementary caption was not provided. Please check suggested data if appropriate and correct if necessary. Please check this box if you have no corrections to make to the PDF file. ☐

Thank you for your assistance.

Graphical abstract

pp. xxx – xxx

Lipid nanocarriers containing a levodopa prodrug with potential antiparkinsonian activity
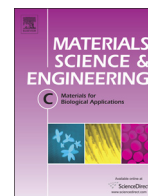
Laura Ravani, Maria Grazia Sarpietro, Elisabetta Esposito, Antonio Di Stefano, Piera Sozio, Mariangela Calcagno, Markus Drechsler, Catia Contado, Francesco Longo, Maria Chiara Giuffrida, Francesco Castelli, Michele Morari, Rita Cortesi *
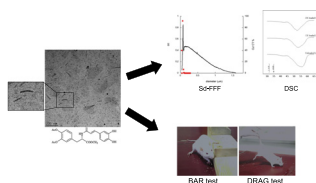
Highlights

Materials Science and Engineering C xxx (2014) xxx–xxx

Lipid nanocarriers containing a levodopa prodrug with potential antiparkinsonian activity

Laura Ravani [a], Maria Grazia Sarpietro [b], Elisabetta Esposito [a], Antonio Di Stefano [c], Piera Sozio [c], Mariangela Calcagno [d,e], Markus Drechsler [f], Catia Contado [g], Francesco Longo [d,e], Maria Chiara Giuffrida [b], Francesco Castelli [b], Michele Morari [d,e], Rita Cortesi [a,*]

[a] *Department of Life Sciences & Biotechnology, University of Ferrara, Ferrara, Italy*
[b] *Department of Drug Sciences, University of Catania, Catania, Italy*
[c] *Department of Pharmaceutical Sciences, University of "G. D'Annunzio", Chieti, Italy*
[d] *Department of Medical Sciences, University of Ferrara, Ferrara, Italy*
[e] *Centre for Neuroscience, National Institute for Neuroscience, University of Ferrara, Ferrara, Italy*
[f] *Macromolecular Chemistry II, University of Bayreuth, Germany*
[g] *Department of Chemical and Pharmaceutical Sciences, University of Ferrara, Ferrara, Italy*
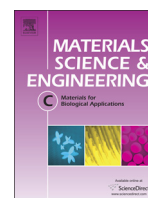
- Formulation of nanocarriers (LN) containing antiparkinsonian L-dopa prodrug (LD-PD)
- DSC showed that the loaded LD-PD interacts with the lipid phase.
- Controlled prodrug release from LD-PD loaded LN confirmed by in vitro studies.
- LD-PD loaded LN reduced parkinsonian disabilities and shows a longer lasting action.

Q3 Supplementary material.

Lipid nanocarriers containing a levodopa prodrug with potential antiparkinsonian activity

Q2 Q1 Laura Ravani [a], Maria Grazia Sarpietro [b], Elisabetta Esposito [a], Antonio Di Stefano [c], Piera Sozio [c], Mariangela Calcagno [d,e], Markus Drechsler [f], Catia Contado [g], Francesco Longo [d,e], Maria Chiara Giuffrida [b], Francesco Castelli [b], Michele Morari [d,e], Rita Cortesi [a,*]

[a] Department of Life Sciences & Biotechnology, University of Ferrara, Ferrara, Italy
[b] Department of Drug Sciences, University of Catania, Catania, Italy
[c] Department of Pharmaceutical Sciences, University of "G. D'Annunzio", Chieti, Italy
[d] Department of Medical Sciences, University of Ferrara, Ferrara, Italy
[e] Centre for Neuroscience, National Institute for Neuroscience, University of Ferrara, Ferrara, Italy
[f] Macromolecular Chemistry II, University of Bayreuth, Germany
[g] Department of Chemical and Pharmaceutical Sciences, University of Ferrara, Ferrara, Italy

ARTICLE INFO

ABSTRACT

This paper describes the production, characterization and in vivo activity of lipid nanocarriers (LN) containing a levodopa prodrug (LD-PD) with therapeutic potential in Parkinson's disease. LD is the mainstay of the pharmacotherapy of Parkinson's disease. However, after a good initial response, motor fluctuations, dyskinesia and loss of efficacy, develop over time, partly due to oscillations in plasma and brain levels of the drug. LD-PD was produced with the aim of prolonging the pharmacological activity of LD. To improve solubility, and simultaneously provide a long lasting release and therapeutic efficacy, the prodrug was formulated in tristearin/lecithin LN. The obtained formulation was homogeneous in particle size and remained stable for up to 2 months from preparation. For the three different tested LD concentrations, namely 1.25, 2.5 and 5.0 mg/ml, the morphological characterization revealed no substantial differences between unloaded and LD-PD loaded LN. The calorimetric test showed an interaction between the lipid phase and the loaded prodrug. In vitro studies using the dialysis method and enzymatic degradation procedure showed that the LD-PD loaded LN provided a controlled prodrug release. Finally, two behavioural tests specific to akinesia (bar test) or akinesia/bradykinesia (drag test) performed in 6-hydroxydopamine hemilesioned mice (a model of Parkinson's disease) demonstrated that the LD-PD loaded LN attenuated parkinsonian disabilities, showing a slightly reduced maximal efficacy but a longer lasting action (up to 24 h) than an equal dose of LD. We conclude that LD-PD loaded LN may represent a future LD formulation useful in Parkinson's disease therapy.

1. Introduction

Parkinson's disease is a neurodegenerative disorder associated with the loss of dopamine neurons in the nigrostriatal system [1]. Current therapy for Parkinson's disease is essentially symptomatic and the gold standard is the natural isomer of the immediate precursor to dopamine, L-3,4-Dihydroxyphenylalanine (L-dopa, LD) [2]. LD is readily transported across the blood–brain barrier (BBB) and converted to dopamine by aromatic L-amino acid decarboxylase. After a good initial response, various complications develop over the course of long-term therapy with LD [3]. Dyskinesia, in particular, is thought to partly depend on the oscillation of plasma levels of the drug, as they appear to be reduced with longer acting LD formulations or dopaminomimetics [4]. In fact, LD is sensitive to peripheral decarboxylation as well as chemical and enzymatic oxidation.

Drug delivery systems (DDS) represent an opportunity in the development of effective treatments for Parkinson's disease since they are able to improve both the pharmacological and therapeutic properties of conventional and new drugs. DDS can be either biodegradable or non-biodegradable, depending on the material used for their preparation. In addition, two main classes of materials should be individuated, namely, polymers and lipids. Among DDS, nanoparticles seem to be effective in facilitating the delivery of small molecules to the brain [5–10].

As an example of polymeric nanoparticles, it has been demonstrated that dopamine-loaded chitosan nanoparticles can improve dopamine

* Corresponding author at: Department of Life Sciences and Biotechnology, University of Ferrara, I-44121 Ferrara, Italy.
  E-mail address: crt@unife.it (R. Cortesi).

transport across the cells [11]. Moreover, LD encapsulated in chitosan nanoparticles and incorporated in poloxamer gel for intranasal delivery has been shown to significantly increase the drug content in the brain [12].

To our knowledge, there are few papers in the literature concerning lipid-based nanoparticles with a specific focus on possible Parkinson's treatment. For instance, one of our previous studies on bromocriptine demonstrated that solid lipid nanoparticles are able to prolong the uptake of bromocriptine and increase its half-life, reducing dyskinesia in rats effectively [13].

Another interesting study conducted by Fernandes and Patravale [14] demonstrated that lipid nanocarriers of LD obtained using supercritical solvents in surfactant solutions can be successfully prepared with a homogenous distribution and more than 90% encapsulation efficiency, thereby contributing to improved stability of the drug against atmospheric oxidation. However, no in vivo experiments were performed with these lipid nanocarriers [14].

The dispersal phase of lipid nanoparticle dispersions is typified by a matrix of crystalline solid lipids, which protects encapsulated molecules from degradation and modulates their release [15–17]. Indeed, lipid nanoparticles seem to allow brain penetration of otherwise non-transportable drugs, masking their physico-chemical characteristics [18–23]. They represent a good delivery system for drug administration offering several clinical advantages, such as the increase of drug bio-availability, the reduction of drug dosage and side effects, and the improvement of patient quality of life [24–26].

Another largely employed strategy to prolong the pharmacological activity of LD and enhance its absorption is typified by the synthesis of LD-based prodrugs. Among these prodrugs, Di Stefano and collaborators have synthesized some compounds providing a relatively slow and constant release of LD in rat and human plasma. Unfortunately, these compounds were characterized by poor water solubility that limited systemic administration [27–29].

In particular, methyl O-acetyl-3-(acetyloxy)-N-[(2E)-3-(3,4-dihydroxyphenyl)prop-2-enoyl]-L-tyrosinate (LD-PD; Fig. 1) was obtained by joining 3,4-diacetyloxy-L-dopa methyl ester with caffeic acid [27–30]. LD-PD showed a good pharmacological profile, but was rapidly degraded in human plasma (half-life of about 6.53 min). A therapeutic advantage of this prodrug might be the targeted delivery of an antioxidant molecule (caffeic acid) to specific cells (such as dopamine neurons) where cellular stress is associated with the pathology [30]. This therapeutic approach appears to be unexplored in the field of Parkinson's disease. Preliminary in vitro and in vivo studies evaluating the chemical and enzymatic properties of this molecule have revealed that LD-PD is stable in aqueous solutions and improves the release of LD and dopamine into the brain [27].

Taking the considerations described above together, our purpose in this study was to investigate the use lipid nanocarriers (LN) as an alternative biocompatible delivery system for administering an LD prodrug. Specifically, a characterization of the LN preparation containing LD-PD in terms of its morphology, dimensions, structural properties and drug distribution was firstly performed. Then, the ability of the LN containing LD-PD to attenuate motor deficits in 6-hydroxydopamine (6-OHDA) hemilesioned mice (a model of Parkinson's disease) was determined in vivo.
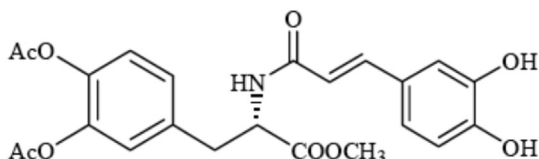

Fig. 1. Chemical structure of LD-PD.

2. Materials and methods

2.1. Materials

Stearic triglyceride (tristearin) was provided by Fluka (Buchs, Switzerland). Lutrol F 68, methyl-oxirane polymer (75;30) (poloxamer 188) was a gift from BASF ChemTrade GmbH (Burgbernheim, Germany). Phospholipon® 90G (P90G), a highly purified soybean lecithin containing at least 90% phosphatidylcholine, was supplied by Rhône-Poulenc-Rorer (Germany). Labrasol®, caprylocaproyl macrogol-8 glycerides, was purchased from Gattefossé (France). Six-hydroxydopamine (6-OHDA) hydrochloride was purchased from Tocris Bioscience (Bristol, UK). LD methyl ester and benserazide were purchased from Sigma (Sigma-Aldrich, AB, Italy). LD and 0 benserazide were dissolved in saline solution (NaCl 0.90% w/v) just prior to use.

2.2. Lipid nanoparticle preparation

LN was prepared by stirring and ultrasonication [13]. Briefly, 0.8 g of tristearin and 0.005 g of soybean phosphatidylcholine were melted at 70 °C. The fused lipid phase was added to 0.2 g of Labrasol®, and the mixture obtained was dispersed in 19 ml of poloxamer 188 solution (2.5% w/w). In turn, LD-PD at 2.5%, 5.0% or 10% by weight with respect to the solid phase was added to the molten mixture of tristearin/soybean phosphatidylcholine/Labrasol®. Afterwards, the mixture was added to the aqueous phase. The obtained emulsion was subjected to ultrasonication (Microson™, Ultrasonic cell Disruptor) at 6.75 kHz for 15 min and then cooled down to room temperature by placing it in a water bath at 22 °C. LN dispersions were stored at room temperature.

2.3. Characterization of lipid nanoparticle dispersions

2.3.1. Photon correlation spectroscopy (PCS)

Submicron particle size analysis was performed using a Zetasizer 3000 PCS (Malvern Instr., Malvern, England) equipped with a 5 mW helium neon laser with a wavelength output of 633 nm. Glassware was cleaned of dust by washing with detergent and rinsing twice with water for injections. Measurements were made at 25 °C at an angle of 90°. Data were interpreted using the "method of cumulants" [31].

2.3.2. Sedimentation field flow fractionation (SdFFF) analysis

An SdFFF system Model S101 (FFFractionation, Inc., Salt Lake City, UT, USA) was employed to determine the size distribution of particles (PSD) by converting the data to graphical results [32]. The mobile phase was deionized water produced by a Milli-Q water (Millipore S.p.A., Vimodrone, Milan, Italy) pumped at 2.0 ml/min and monitored on each run. Fifty microlitre samples were injected through a 50 μl Rheodyne loop valve.

The automatic collection of the fractions (every 90 s) was performed using a Bio Rad Model 2110 fraction collector (Bio Rad laboratories, UK) positioned at the end of the SdFFF system. The volume of each fraction was 3 ml.

2.3.3. Cryo-transmission electron microscopy (Cryo-TEM)

Samples were vitrified as previously described [13,33], and transferred to a Zeiss EM922 transmission electron microscope for imaging using a cryoholder (CT3500, Gatan). The temperature of the sample was kept below −175 °C throughout the examination. Specimens were examined with doses of about 1000–2000 e/nm² at 200 kV. Images were digitally recorded by a CCD camera (Ultrascan 1000, Gatan) using an image processing system (GMS 1.4 software, Gatan).

2.3.4. FTIR studies

The spectra of pure LD-PD, excipients containing 10% of LD-PD, empty LN, and LD-PD loaded LN were run on a Perkin-Elmer FTIR

1600 spectrometer (Monza, Italy). The scanning range was 400–4000 cm^{-1}. Samples were prepared as KBr pellets.

2.3.5. Differential scanning calorimetry (DSC) measurements

DSC measurements were performed using a Mettler Toledo STAR^e system equipped with a DSC-822^e calorimetric cell and Mettler TA-STAR^e software. The maximum possible sensitivity was automatically chosen by the calorimetric system, and the reference pan was filled with bidistilled water. The calorimetric system was calibrated, in transition temperature and enthalpy changes, by using indium, stearic acid and cyclohexane, following the procedure of the DSC 822 Mettler TA STAR^e instrument.

Eighty microlitres of LP-PD-containing LN was taken from the bulk, put into the calorimetric pan, hermetically sealed and subjected to heating and cooling scans for at least three times as follows: (i) a scan from 5 to 65 °C (2 °C/min); and (ii) a scan from 65 to 5 °C (4 °C/min).

2.4. Drug content of dispersions

With the aim of quantifying the drug content (free plus bound) of dispersions after production, a sample of dispersion was diluted in methanol (1:5 v/v) and stirred for 3 h in order to completely extract LD-PD. Afterwards, the sample was filtered through 0.22 μm nylon filter (Spartan 13, Whatman, Germany) and analysed by HPLC for LD-PD content.

The HPLC determinations were performed using a two-plunger alternative pump (Jasco, Japan), a UV detector operating at 254 nm and a 7125 Rheodyne injection valve with a 50 μl loop. Forty microlitre samples were loaded onto a stainless steel C-18 reverse-phase column (15 × 0.46 cm) packed with 5 μm particles (Hypersil BDS, Alltech, USA). Elution was performed with a mobile phase constituted of methanol and water (60:40 v/v) at a flow rate of 0.5 ml/min. In these conditions, the retention time of LD-PD was 5.4 min.

The drug content of the dispersion was calculated by applying the following equation:

$$\text{Drug recovery} = \text{amount of drug detected by HPLC} \times 100/\text{total amount of drug employed}.$$

Data were the mean of 8 determinations for each batch of LN type.

2.5. In vivo tests

The adopted experimental protocols were approved by the Italian Ministry of Health (licence no. 171/2010-B) and by the Ethical Committee of Ferrara University. Adequate measures were taken to minimize animal pain and discomfort and to limit the number of animals employed in the study. Mice were kept under regular lighting conditions (12 h light/dark cycle) and given food and water ad libitum.

2.5.1. Unilateral lesion with 6-hydroxydopamine

Unilateral lesion of nigral dopaminergic neurons was stereotaxically induced in isoflurane-anaesthetized C57BL/6 mice (25 g; Harlan Italy, San Pietro al Natisone, Italy), as previously described [34]. Mice received two injections × 2 μl of 6-OHDA (3.0 μg/μl freebase, dissolved in saline with 0.02% ascorbic acid) into the striatum at the following coordinates from bregma: (i) AP + 1.0, L − 2.1, DV − 2.9; and (ii) AP + 0.3, L − 2.3, DV − 2.9 [35]. In order to assess the degree of dopamine depletion, all mice were tested for spontaneous rotation, and for akinesia/bradykinesia (bar and drag tests) 10 days after lesion [34].

2.5.2. Behavioural studies

Motor activity was evaluated in hemiparkinsonian mice using two tests specific for different motor abilities [34,36,37]: (i) the "bar test", which measures the ability of the mouse to respond to an externally imposed static posture [38]; (ii) the "drag test" (modification of the "wheelbarrow" test) [39], which measures the ability of the mouse to balance its body posture using forelimbs in response to an externally imposed dynamic stimulus (backward dragging). The two tests were repeated in the same sequence, with the first test always being the bar test.

2.5.3. Experimental design

Prior to pharmacological testing, the mice were handled for 1 week by the same operator to reduce stress, and trained daily for an additional week on the behavioural tests until their motor performance became reproducible. Eight 6-OHDA hemilesioned mice were divided into two groups receiving LD or LD-PD loaded LN (LD content equal to 10 mg/kg or 0.05 mmol/kg), and 3 days later the same groups were treated with vehicle or saline. The same protocol was repeated a week later crossing the treatments. Drugs were administered systemically (i.p.). LD or LD-PD loaded LN administration was preceded (10 min) by a systemic (i.p.) injection of benserazide (12 mg/kg or 0.05 mmol/kg). Each experiment consisted of six consecutive sessions carried out under drug-free conditions (baseline, control session), and 20, 90, 180, 360 min and 24 h after drug, saline or vehicle administration.

2.5.4. Data presentation and statistical analysis

Data were expressed as means ± SEM of eight determinations per group. Motor performance was expressed as absolute values (seconds of immobility in the bar test, and number of steps in the drag test). Statistical analysis was performed (GraphPad Software, Inc., Lajolla, CA) by 1-way repeated measure (RM) ANOVA followed by the Bonferroni post hoc test, or by the Student t-test when only two groups were compared.

3. Results and discussion

3.1. Production and characterization of LD-PD containing LN

LN were prepared using increasing amounts of LD-PD, namely, 1.25 (0.5×), 2.5 (1×; reference preparation) and 5 (2×) mg/ml.

Cryo-transmission electron microscopy was used to investigate the morphology of the particles in LN dispersions. Fig. 2 reports cryo-TEM images of empty and 1× LD-PD loaded LN, taken as example. The roundish dark spots (indicated by some closed arrows) are ice crystals.

In general, LN dispersions are heterogeneous and mainly constituted of discoid-shaped structures; thus, when viewed edge-on, the particles appear as circular or ellipsoidal, or as dark rods or "needles", depending on particle position and on their thickness. The thickness of rod- or needle-like particles in the electron micrographs is around 10 nm. A precise value could not be calculated because the tilt of the particles cannot be exactly determined. However, it is worth mentioning that the LN structure was not affected by LD-PD, even at the other tested concentrations (data not shown).

At the higher magnification structures in the form of a "crescent" evidence the inner lamellar morphology of nanoparticles, probably due to the presence of tristearin assembled with the mixture of soybean phosphatidylcholine and Labrasol®, resulting in the typical "sandwich-like" appearance.

Moreover, in Fig. 2B the presence of LD-PD gives rise to a more homogeneous particle population with respect to empty LN, possibly suggesting the prodrug's role as surfactant agent.

The interaction between LD-PD and LN was studied using an FT-IR spectrometer. The FT-IR spectra of LD-PD showed − NH stretch at 3404.3 cm^{-1} and − C═O stretch 1654.8 cm^{-1} while FT-IR spectra of LD-PD loaded LN displayed − NH stretch at 3478.5 cm^{-1} and − C═O stretch 1657.6 cm^{-1} (see Fig. S1 and Table 1). A shift in the − NH and − C═O stretch indicates the involvement of these functional groups in the interaction between LD-PD and LN as reported by Rohit and Pal [40]. In LD-PD loaded LN we observed a shift in − NH stretching and also in − C═O stretching suggesting favourable interactions possibly
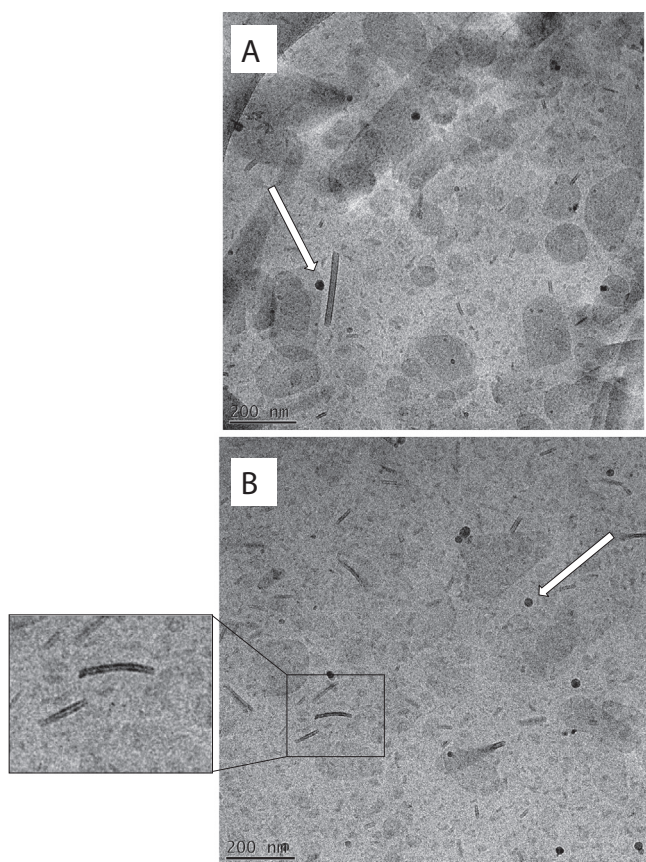
Fig. 2. Cryo-transmission electron microscopy images of unloaded (A) and 1× LD-PD loaded LN (B).

Fig. 3. PSDs elaborated from the SdFFF fractograms. LN particles were assumed to have a density of 0.0646 g/ml (d = diameter of the equivalent sphere; dd = dimensional distribution, i.e. mass frequency function). The squared symbols indicate LD-PD content, as determined by HPLC.

improving the entrapment efficiency of this LD prodrug in lipid nanoparticle dispersions.

The LN size was measured immediately after the production and up to 4 months later, in order to evaluate the stability of formulations. Table 1 shows that 2× LD-PD loaded LN is characterized by the smallest size compared to the other LD-PD loaded LN, and confirms the heterogeneity of the nanoparticle populations evidenced from cryo-TEM images. However, 4 months after production, no dimensional changes were observed, and the 1× LD-PD loaded LN result was the most stable.

Due to the crushed and flat form of LN, the 1× LD-PD loaded LN (taken as a reference) was subjected to SdFFF analysis. Fig. 3 presents an example of a particle-size distribution plot achieved from this type of chromatographic-like analysis [33,41]. Around the 80% of the nanoparticle population belongs to the main peak at roughly 160 nm, which is in very good agreement with the sizes determined by PCS and reported in Table 2. The very thin peak at 80 nm is due to the particles that are smaller than 100 nm, which exit the channel all together, only partially resolved from the void peak.

SdFFF was also employed to obtain information about LD-PD encapsulation. The amount of LD-PD encapsulated in the LN was determined by HPLC after diluti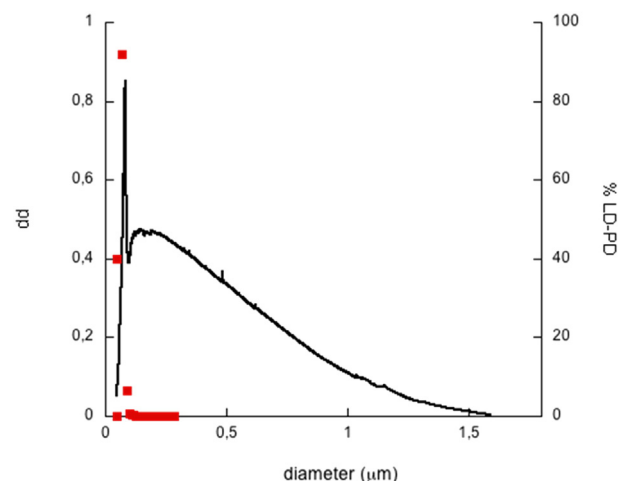ng with the mobile phase, by injecting the eluate exiting from the SdFFF channel collected during the fractionation. The injection results of the reference preparation of 1× LD-PD loaded LN are reported in Fig. 3 (square dots), where it is clearly evident that the LD-PD is entirely associated with nanoparticles.

However, compared to the initially weighed amount of LD-PD, the final content within the LN dispersions, as determined by HPLC and summarized in Table 2, indicates that the prodrug's recovery is the highest in the 0.5× LD-PD loaded LN (83.03%), intermediate in the 1× LD-PD loaded LN (71.21%) and the lowest in 2× LD-PD-loaded LN (43.36%). We therefore hypothesize that during the manufacturing process a significant quantity of prodrug is lost (probably in the lipid phase along the wall of the flask) due to the larger amount of LD-PD incorporated within the limited amount of lipid phase. In order to prove this, an extraction of LD-PD from the lipid phase adhering to the surfaces of both the vessel and the homogenizer's blade was performed following the procedures described above for the determination of drug content. The results, which are reported in Table 3, confirmed our assumption.

3.2. Calorimetric studies

It is well known that structural alterations of materials are accompanied by heat exchanges, such as the uptake of heat during melting or the emission of heat during crystallization. DSC allows thermal events in the sample to be monitored and quantified, and the temperatures at which these events occur to be identified [42–45], thus providing information on the structural properties of a sample. Fig. 4 reports the calorimetric curves, in heating mode, of unloaded and LD-PD loaded LN.

The calorimetric curve of unloaded LN is characterized by a main peak at 56.4 °C and three shoulders at lower temperatures, namely, 43.0 °C, 49.0 °C and 53.5 °C. The 1× LD-PD loaded LN shows five calorimetric signals: a small peak at about 43.0 °C, two shoulders at 46.0 and 50.0 °C, respectively, a main peak at 53.0 °C and a shoulder at about 57.0 °C. The calorimetric scan of the 2× LD-PD loaded LN was similar to that of the

Table 1
FT-IR data of LD-PD and LD-PD loaded LN.

	Observed value (cm^{-1})	Expected values (cm^{-1})	Functional group	Attribution
LD-PD	3404.3	3500–3100	NH amide	N–H stretch
	1654.8	1690–1640	C=O amide	C–O stretch
	1600.8	1640–1550	NH amide	NH bending
LD-PD loaded LN	3478.5	3500–3100	NH amide	N–H stretch
	1657.6	1690–1640	C=O amide	C–O stretch
	1590.7	1640–1550	NH amide	NH bending

Table 2

Mean diameters of LD-PD loaded LN as determined by PCS.

Day	Mean diameter (nm) ± s.d.					
	0.5× LD-PD loaded LN	Polydispersity ± s.d.	1× LD-PD loaded LN	Polydispersity ± s.d.	2× LD-PD loaded LN	Polydispersity ± s.d.
0	158.8 ± 2.2	0.27 ± 0.02	161.9 ± 0.8	0.26 ± 0.04	149.9 ± 3.2	0.26 ± 0.01
30	152.85 ± 0.9	0.30 ± 0.01	164.5 ± 3.7	0.29 ± 0.02	147.2 ± 2.8	0.23 ± 0.03
120	151.7 ± 3.4	0.28 ± 0.04	160.5 ± 2.4	0.30 ± 0.02	146.1 ± 0.8	0.29 ± 0.02

s.d. = standard deviation.

Data are the mean of 5 determinations on different batches of the same type of dispersion.

1× LD-PD loaded LN, the only exception being the loss of the shoulder at higher temperature. The comparison of the calorimetric scans of unloaded and LD-PD loaded LN provided important information. The unloaded LN scan shows interesting differences from the loaded scan, with the exception of the small peak at about 43.0 °C present in both unloaded and loaded LN. In comparison with unloaded LN, the main peak of the loaded LN is moved towards a lower temperature. In 1× LD-PD loaded LN, two shoulders are present at about 50.5 and 57.0 °C, respectively. In 2× LD-PD loaded LN, only the shoulder at about 50.5 °C is visible. In addition, the peak intensity decreases, going from unloaded to 2× LD-PD loaded LN. The results obtained clearly indicate that LD-PD affects the thermotropic behaviour of LN and that the effect is related to the amount of prodrug loaded. This evidence is strengthened by the enthalpy values as a function of LD-PD within LN (data not shown). The enthalpy decreases when the amount of prodrug within the LN is increased. These data suggest that the prodrug becomes distributed inside the LN and this causes a decrease of the lipid molecules cooperativeness.

Additional studies were conducted to evaluate if LD-PD or its moieties (i.e. caffeic acid and diacetyl dopa) are absorbed by LN (see Supplementary Data section). The results obtained (Fig. S2) allowed us to demonstrate that the simple contact between compounds and LN does not cause their absorption by unloaded LN, hence confirming the feasibility of loading LD-PD into LN.

On the basis of the morphological results, the reference formulation was selected for the in vitro and in vivo studies. The in vitro studies, reported in the "Supplementary Data" section of the present article, indicate that the inclusion of LD-PD in LN not only facilitates its dissolution in aqueous media but also represents a source for the long lasting release of the prodrug. In addition, considering that LD-PD has to be bioactivated to LD to exert its pharmacological activity after in vivo administration, the degradation kinetics of 1× LD-PD loaded LN was investigated in the presence of FCS esterases [46]. The results obtained indicated that LN is able to increase LD-PD's half-life by 3.5-fold (data not shown).

3.3. In vivo studies

Due to its low solubility in water (or aqueous solution), LD-DP administration is very difficult — generally significant amounts of surfactants have to be used. However, this would result in significant toxicity and impairment of animal performance in vivo. Therefore, in vivo studies were performed comparing the antiparkinsonian activity of LD-PD loaded LN with that of LD, administered as an equivalent LD dose.

Six-OHDA hemilesioned mice showed marked akinesia and bradykinesia, mainly affecting the forepaw contralateral to the toxin injection side. Indeed, the time spent on the bars with the contralateral (parkinsonian) paw (45.2 ± 2.7 s) was greater than that with the ipsilateral paw (28.0 ± 4.3 s; p < 0.01, Student's t-test). Moreover the contralateral forepaw performed a reduced number of steps (2.2 ± 0.3) compared to the ipsilateral one (14.8 ± 1.1; p < 0.01, Student's t-test). LD was systemically administered (i.p.) at a dose (10 mg/kg or 0.05 mmol/kg, in combination with 12 mg/kg benserazide) that was reported to attenuate hypokinesia in MPTP-treated [36] or 6-OHDA hemilesioned [34] mice. LD reduced the immobility time (Fig. 5A) and increased the number of steps (Fig. 5C) at the contralateral paw. The reduction of immobility time peaked at 20 min after injection (−75%), was close to maximal at 120 min (−70%), was still significant after 3 h (−32%), but vanished after 6 h. A similar pattern was observed in the drag test, where an approximately fourfold increase in stepping within the 20–90 min time window was observed. The improvement was still remarkable (threefold) after 3 h, but vanished after 6 h.

LD-PD loaded LN (0.05 mmol/kg in terms of LD content) replicated the effect of LD in both tests, showing a slightly reduced maximal efficacy accompanied by a longer lasting action. In the bar test (Fig. 5A), the effect of this LD formulation was evident after 20 min (−32%), peaked after 90 min (−45%), was still close to maximal after 3 h (−37%), but vanished after 6 h.

In the drag test (Fig. 5C), the stepping-improving effect of LD-PD-loaded LN was significant after 20 min (threefold), peaked at 90 min (fourfold), was still maximal after 3 h and was different from LD alone, and still remarkable between 6 and 24 h from administration (threefold).

We also monitored the effects of LD at the ipsilateral forepaw. LD alone reduced the immobility time within the 20–90 min time-window (−50%), but not at later time points (Fig. 5B). Likewise, a

Table 3

LD-PD recovery after LN production.

LD-PD loaded LN	LD-PD % recovery in LN ± s.d.	LD-PD % recovery in vessel/blade ± s.d.
0.5×	83.01 ± 9.38	12.04 ± 1.22
1×	71.21 ± 7.76	21.28 ± 4.31
2×	43.36 ± 6.63	52.72 ± 8.67

The reported results represent the average of four independent experiments ± s.d.
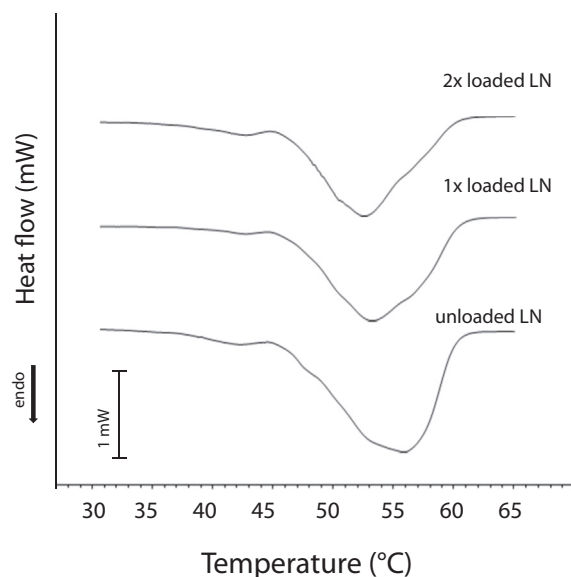
Fig. 4. Calorimetric curves in heating mode of unloaded LN, 1×-LD-PD-loaded and 2×-LD-PD loaded.
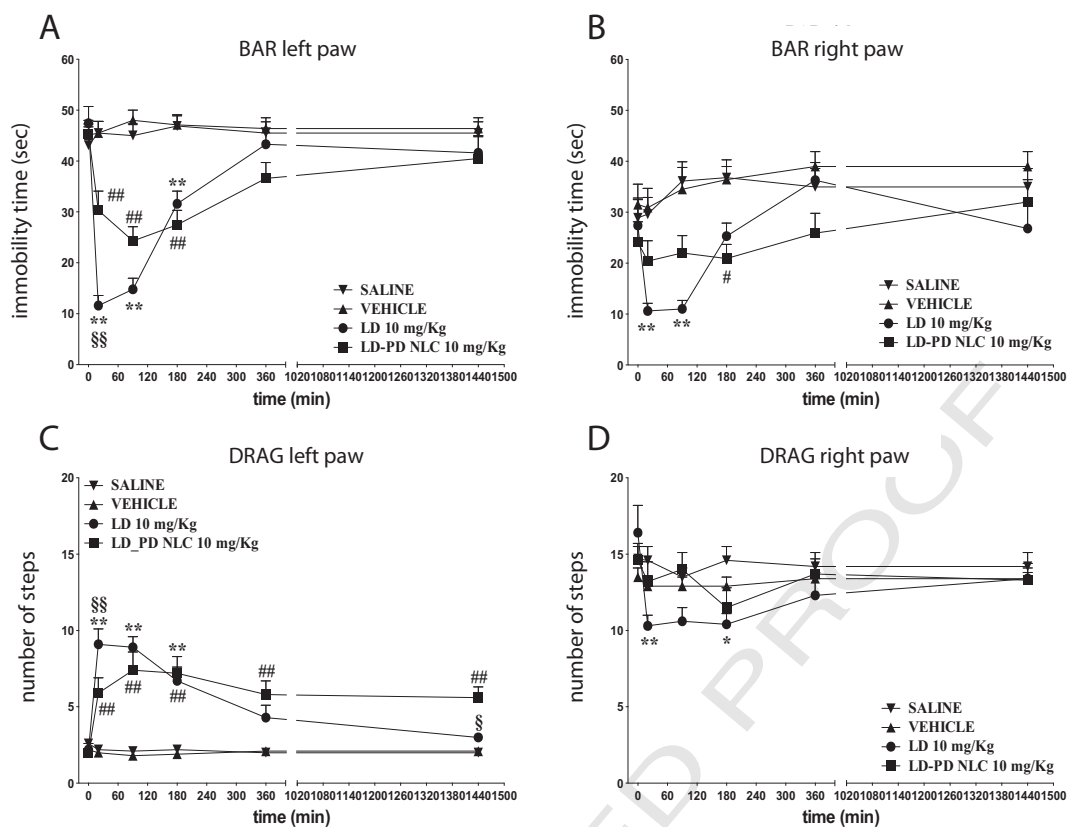
Fig. 5. In vivo experiments showing the effects of L-Dopa (LD, ●), LD-PD loaded LN (LD-PD LN, ■) and controls (saline ▼, and vehicle ▲, respectively) evaluated as immobility time in the bar test (A, B) and number of steps in the drag test (C, D). LD-PD LN was administered at the same equivalent dose of LD (10 mg/Kg, 0.05 mmol/Kg). Benserazide (12 mg/Kg) was administered 5 min before LD and LD-PD LN. Data are means ± SEM of n = 8 determinations per group. *p < 0.05, **p < 0.01 different from saline; # < 0.05, ## < 0.01 = different from vehicle (empty LN); § < 0.05, §§ < 0.01 different from LD-PD LN (1-way RM ANOVA followed by the Bonferroni test).

reduction of stepping was observed within the 20–180 min time window (−30%; Fig. 5D). LD-PD loaded LN exerted only mild effects at the ipsilateral paw. A reduction of immobility time was observed 180 min after injection (Fig. 5B). Moreover, LD-PD loaded LN did not affect stepping activity at the ipsilateral paw (Fig. 5D).

These data clearly indicate the high potential of LD-PD as a compound to reverse the impairment of voluntary motor activity and the abnormal slowness of movement associated with experimental parkinsonism. Compared to the same dose of LD, the therapeutic benefit of LD-PD was extended by up to 24 h, particularly in the stepping test, a test more closely related to the striatal sensory-motor function [47]. This suggests that the inclusion of LD-PD within LN improves its water solubility, allowing for a reduction of the dosage. This formulation might also cause a prolongation of therapeutic concentrations of LD within the brain. This might be related to a prolonged release of the prodrug along with a longer stability of LN in the blood. Indeed, LN produced in the presence of poloxamer 188 may behave as a "stealth carrier", being somewhat protected by opsonization [48,49].

4. Conclusions

LD is the gold standard in the treatment of Parkinson's disease, but its use is associated with some problems, such as fast metabolism and motor complications. As the disease progresses the frequency of LD administration is increased, leading to a complex treatment schedule with poor patient compliance. The development of long acting formulations ensuring continuous delivery is therefore of crucial importance. In the present study, we have proved the feasibility of producing LN to carry a LD prodrug. The produced formulation showed good characteristics in terms of size and morphology, remaining stable up to 2 months from preparation. In vitro studies showed that LP-PD stably interacted

with the lipid phase of LN from where it was released. In vivo tests demonstrated that LP-PD loaded LN replicated the therapeutic benefit of LD, with a slightly reduced maximal efficacy but a longer lasting action (up to 24 h). Although some improvement in the lipid composition of these LN is needed, in conjunction with more thorough pharmacokinetic studies, to fully understand the in vivo behaviour of this novel formulation, these data provide evidence for the long lasting antiparkinsonian activity of a novel LD prodrug.

Appendix A. Supplementary data

Supplementary data to this article can be found online at http://dx.doi.org/10.1016/j.msec.2014.12.014.

References

[1] P.A. Serra, G. Esposito, P. Enrico, M.A. Mura, R. Migheli, M.R. Delogu, M. Miele, M.S. Desole, G. Grella, E. Miele, Manganese increases L-DOPA auto-oxidation in the striatum of the freely moving rat: potential implications to L-DOPA long-term therapy of Parkinson's disease, Br. J. Pharmacol. 130 (2000) 937–945.

[2] E. Tolosa, M.J. Marti, F. Valldeoriola, J.L. Molinuevo, History of levodopa and dopamine agonists in Parkinson's disease treatment, Neurology 50 (1998) S2–S10.

[3] W.C. Koller, Neuroprotective therapy for Parkinson's disease, Exp. Neurol. 144 (1997) 24–28.

[4] P. Huot, T.H. Johnston, J.B. Koprich, S.H. Fox, J.M. Brotchie, The pharmacology of L-DOPA-induced dyskinesia in Parkinson's disease, Pharmacol. Rev. 65 (2013) 171–222.

[5] S. Md, R.A. Khan, G. Mustafa, K. Chuttani, S. Baboota, J.K. Sahni, J. Ali, Bromocriptine loaded chitosan nanoparticles intended for direct nose to brain delivery: pharmacodynamic, pharmacokinetic and scintigraphy study in mice model, Eur. J. Pharm. Sci. 48 (2012) 393–405.

[6] M.J. Tsai, Y.B. Huang, P.C. Wu, Y.S. Fu, Y.R. Kao, J.Y. Fang, Y.H. Tsai, Oral apomorphine delivery from solid lipid nanoparticles with different monostearate emulsifiers: pharmacokinetic and behavioral evaluations, J. Pharm. Sci. 100 (2011) 547–557.

[7] M. Fernandez, E. Barcia, A. Fernandez-Carballido, L. Garcia, K. Slowing, S. Negro, Controlled release of rasagiline mesylate promotes neuroprotection in a rotenone-induced advanced model of Parkinson's disease, Int. J. Pharm. 438 (2012) 266–278.

[8] K. Hu, Y. Shi, W. Jiang, J. Han, S. Huang, X. Jiang, Lactoferrin conjugated PEG-PLGA nanoparticles for brain delivery: preparation, characterization and efficacy in Parkinson's disease, Int. J. Pharm. 415 (2011) 273–283.

[9] Z. Wen, Z. Yan, K. Hu, Z. Pang, X. Cheng, L. Guo, Q. Zhang, X. Jiang, L. Fang, R. Lai, Odorranalectin-conjugated nanoparticles: preparation, brain delivery and pharmacodynamic study on Parkinson's disease following intranasal administration, J. Control. Release 151 (2011) 131–138.

[10] K.B. Kurakhmaeva, I.A. Djindjikhashvili, V.E. Petrov, V.U. Balabanyan, T.A. Voronina, S.S. Trofimov, J. Kreuter, S. Gelperina, D. Begley, R.N. Alyautdin, Brain targeting of nerve growth factor using poly(butyl cyanoacrylate) nanoparticles, J. Drug Target. 17 (2009) 564–574.

[11] E. De Giglio, A. Trapani, D. Cafagna, L. Sabbatini, S. Cometa, Dopamine-loaded chitosan nanoparticles: formulation and analytical characterization, Anal. Bioanal. Chem. 400 (2011) 1997–2002.

[12] S. Sharma, S. Lohan, R.S. Murthy, Formulation and characterization of intranasal mucoadhesive nanoparticulates and thermo-reversible gel of levodopa for brain delivery, Drug Dev. Ind. Pharm. 40 (2014) 869–878.

[13] E. Esposito, M. Fantin, M. Marti, M. Drechsler, L. Paccamiccio, P. Mariani, E. Sivieri, F. Lain, E. Menegatti, M. Morari, R. Cortesi, Solid lipid nanoparticles as delivery systems for bromocriptine, Pharm. Res. 25 (2008) 1521–1530.

[14] C.B. Fernandes, V.B. Patravale, Fabrication of lipid nanocarriers of levodopa using supercritical fluid technology, Proceedings of 10th International Symposium on Supercritical Fluids (ISSF 2012), San Francisco, CA, USA, 2012.

[15] W. Mehnert, K. Mäder, Solid lipid nanoparticles: production, characterization and applications, Adv. Drug Deliv. Rev. 47 (2001) 165–196.

[16] G.M. Barratt, Therapeutic applications of colloidal drug carriers, Pharm. Sci. Technol. Today 3 (2000) 163–171.

[17] M. Harms, C.C. Muller-Goymann, Solid lipid nanoparticles for drug delivery, J. Drug Deliv. Sci. Technol. 21 (2011) 89–99.

[18] E. Barbu, É. Molnàr, J. Tsibouklis, D.C. Górecki, The potential for nanoparticle-based drug delivery to the brain: overcoming the blood–brain barrier, Expert Opin. Drug Deliv. 6 (2009) 553–565.

[19] S. Pasha, K. Gupta, Various drug delivery approaches to the central nervous system, Expert Opin. Drug Deliv. 7 (2010) 113–135.

[20] V. Kabanov, E.V. Batrakova, New technologies for drug delivery across the blood brain barrier, Curr. Pharm. Des. 10 (2004) 1355–1363.

[21] K. Andrieux, P. Couvreur, Polyalkylcyanoacrylate nanoparticles for delivery of drugs across the blood–brain barrier, Nanomed. Nanobiotech. 1 (2009) 463–474.

[22] I.P. Kaur, R. Bhandari, S. Bhandari, V. Kakkar, Potential of solid lipid nanoparticles in brain targeting, J. Control. Release 127 (2008) 97–102.

[23] A. Di Stefano, P. Sozio, A. Iannitelli, L.S. Cerasa, New drug delivery strategies for improve Parkinson's disease therapy, Expert Opin. Drug Deliv. 6 (2009) 389–404.

[24] M.D. Joshi, R.H. Müller, Lipid nanoparticles for parenteral delivery of actives, Eur. J. Pharm. Biopharm. 71 (2009) 161–172.

[25] J. Kreuter, Nanoparticles — a historical perspective, Int. J. Pharm. 331 (2007) 1–10.

[26] A.S. Hoffman, The origins and evolution of "controlled" drug delivery systems, J. Control. Release 132 (2008) 153–163.

[27] P. Sozio, A. Iannitelli, L.S. Cerasa, I. Cacciatore, C. Cornacchia, G. Giorgioni, M. Ricciutelli, C. Nasuti, F. Cantalamessa, A. Di Stefano, New L-dopa codrugs as potential antiparkinson agents, Arch. Pharm. 341 (2008) 412–417.

[28] F. Pinnen, I. Cacciatore, C. Cornacchia, P. Sozio, L.S. Cerasa, A. Iannitelli, C. Nasuti, F. Cantalamessa, D. Sekar, R. Gabbianelli, M.L. Falcioni, A. Di Stefano, Codrugs linking L-dopa and sulfur-containing antioxidants: new pharmacological tools against Parkinson's disease, J. Med. Chem. 52 (2009) 559–563.

[29] G. Giorgioni, F. Claudi, S. Ruggieri, M. Ricciutelli, G.P. Palmieri, A. Di Stefano, P. Sozio, L.S. Cerasa, A. Chiavaroli, C. Ferrante, G. Orlando, R.A. Glennon, Design, synthesis, and preliminary pharmacological evaluation of new imidazolines as l-dopa prodrugs, Bioorg. Med. Chem. 18 (2010) 1834–1840.

[30] M. Rosini, V. Andrisano, M. Bartolini, M.L. Bolognesi, P. Hrelia, A. Minarini, A. Tarozzi, C. Melchiorre, Rational approach to discover multipotent anti-Alzheimer drugs, J. Med. Chem. 48 (2005) 360–363.

[31] R. Pecora, Dynamic light scattering measurement of nanometer particles in liquids, J. Nanoparticle Res. 2 (2000) 123–131.

[32] C. Contado, G. Blo, F. Fagioli, F. Dondi, R. Beckett, Characterisation of River Po particles by sedimentation field-flow fractionation coupled to GFAAS and ICPMS, Colloids Surf. A Physicochem. Eng. Asp. 120 (1997) 47–59.

[33] E. Esposito, P. Mariani, L. Ravani, C. Contado, M. Volta, S. Bido, M. Drechsler, S. Mazzoni, E. Menegatti, M. Morari, R. Cortesi, Nanoparticulate lipid dispersions for bromocriptine delivery: characterization and in vivo study, Eur. J. Pharm. Biopharm. 80 (2012) 306–314.

[34] S. Bido, M. Marti, M. Morari, Amantadine attenuates levodopa-induced dyskinesia in mice and rats preventing the accompanying rise in nigral GABA levels, J. Neurochem. 118 (2011) 1043–1055.

[35] G. Paxinos, K.B.J. Franklin, The Mouse Brain in Stereotaxic Coordinates, 2nd ed. Academic Press, San Diego, CA, 2001.

[36] M. Marti, F. Mela, M. Fantin, S. Zucchini, J.M. Brown, J. Witta, M. Di Benedetto, B. Buzas, R.K. Reinscheid, S. Salvadori, R. Guerrini, P. Romualdi, S. Candeletti, M. Simonato, B.M. Cox, M. Morari, Blockade of nociceptin/orphanin FQ transmission attenuates symptoms and neurodegeneration associated with Parkinson's disease, J. Neurosci. 95 (2005) 9591–9601.

[37] R. Viaro, R. Sanchez-Pernaute, M. Marti, C. Trapella, O. Isacson, M. Morari, Nociceptin/orphanin FQ receptor blockade attenuates MPTP-induced parkinsonism, Neurobiol. Dis. 30 (2008) 340–348.

[38] P.R. Sanberg, M.D. Bunsey, M. Giordano, A.B. Norman, The catalepsy test: its ups and downs, Behav. Neurosci. 102 (1988) 748–751.

[39] T. Schallert, M. De Ryck, I.Q. Whishaw, V.D. Ramirez, P. Teitelbaum, Excessive bracing reactions and their control by atropine and L-DOPA in an animal analog of Parkinsonism, Exp. Neurol. 64 (1979) 33–43.

[40] B. Rohit, K.I. Pal, A method to prepare solid lipid nanoparticles with improved entrapment efficiency of hydrophilic drugs, Curr. Nanosci. 9 (2013) 211–220.

[41] M. Blanda, P. Reschiglian, F. Dondi, R. Beckett, Characterization of low-density polybutadiene latexes by sedimentation field-flow fractionation, Polym. Int. 33 (1994) 61–69.

[42] H. Bunjes, T. Unruh, Characterization of lipid nanoparticles by differential scanning calorimetry, X-ray and neutron scattering, Adv. Drug Deliv. Rev. 59 (2007) 379–402.

[43] L. Montenegro, A. Campisi, M.G. Sarpietro, C. Carbone, R. Acquaviva, G. Raciti, G. Puglisi, In vitro evaluation of idebenone-loaded solid lipid nanoparticles for drug delivery to the brain, Drug Dev. Ind. Pharm. 37 (2011) 737–746.

[44] L. Montenegro, S. Ottimo, G. Puglisi, F. Castelli, M.G. Sarpietro, Idebenone loaded solid lipid nanoparticles interact with biomembrane models: calorimetric evidence, Mol. Pharm. 9 (2012) 2534–2541.

[45] L. Montenegro, M.G. Sarpietro, S. Ottimo, G. Puglisi, F. Castelli, Differential scanning calorimetry studies on sunscreen loaded solid lipid nanoparticles prepared by the phase inversion temperature method, Int. J. Pharm. 415 (2011) 301–306.

[46] L. Ravani, E. Esposito, A. Costenaro, M. Drechsler, P. Sozio, A. Di Stefano, R. Cortesi, Lipid Nanocarriers as Delivery Systems for L-dopa Prodrugs: A Comparative Study, 2014. (Unpublished results).

[47] D. Kirik, C. Rosenblad, A. Bjorklund, Characterization of behavioral and neurodegenerative changes following partial lesions of the nigrostriatal dopamine system induced by intrastriatal 6-hydroxydopamine in the rat, Exp. Neurol. 152 (1998) 259–277.

[48] S.M. Moghimi, C. Hunter, J.C. Murray, Long-circulating and target-specific nanoparticles: theory to practice, Pharmacol. Rev. 53 (2001) 283–318.

[49] S.M. Moghimi, C. Hunter, Poloxamers and poloxamines in nanoparticle engineering and experimental medicine, Trends Biotechnol. 18 (2000) 412–420.